Piecewise linear sheet control in an H infinity framework

16th IEEE International Conference on Control Applications
Part of IEEE Multi-conference on Systems and Control
Singapore, 1-3 October 2007

Piecewise Linear Sheet Control in an H_∞ Framework[1]

Jeroen de Best, Björn Bukkems, René van de Molengraft, and Maarten Steinbuch

Abstract— **This paper presents a control design approach for sheet control in a printer paper path. By splitting up the control problem in two levels, i.e. low level motor control loops and a high level sheet control loop, a hierarchical control structure is obtained. The high level sheet dynamics are formulated in the piecewise linear modeling formalism. Given this model, together with models of the controlled low level motor dynamics, a high level feedback controller is designed with guaranteed H_∞ performance. The designed controller is implemented on a experimental paper path setup to show the effectiveness of the control design in practice.**

I. Introduction

Driven by the growing interest for higher productivity of cut sheet printers without loss of accuracy, manufacturers are facing the complex problem of designing sheet handling mechanisms for printer paper paths.

An example of an industrial printer paper path is shown in Fig. 1. The sheets are fed from a high-capacity feeder, here referred to as paper input module (PIM). They are transported to the image transfer section (ITS) where the sheet meets its corresponding image. For the purpose of creating backside prints, the paper path can be equipped with a duplex loop. After being printed, the sheets are transported to the finisher (FIN) where they are collected. The transportation is carried out via so called pinches, which consist of a driven roller and a non-driven roller. The non-driven roller applies sufficient normal force in order to prevent the sheets from slipping in the pinch. The pinches can be driven by motors individually, or they can be grouped together into sections.

In order to achieve a good printing quality the sheet handling mechanism must deliver the sheets in time and with the right velocity at the ITS. In today's cut sheet printers the transportation of the sheets mainly relies on event-driven sheet control in combination with closed-loop motor control. At discrete points in the paper path the presence of a sheet can be detected by sheet sensors. With these measurements the motor velocities can be adjusted in order to correct for possible errors. Together with a high precision mechanical design with small manufacturing tolerances a predictable sheet flow results. However, as consumers demand a higher productivity, the problem faced is to design a printer paper path capable of producing a larger quantity of prints without loss of printing accuracy and without an increase of the cost price. One approach to tackle this problem is to manufacture mechanics with smaller tolerances. In most cases, however, this leads to an increase of the cost price. Another way to solve the problem is to exploit the power of continuous closed-loop sheet feedback control. Known results on sheet feedback control can be found in [1], [2] and [3], where the control design is done intuitively and does not take into account the controlled motor dynamics that will limit the attainable bandwidth. Neither do they take into account the presence of disturbances and uncertainties such as uncertain pinch radii. In [4], we have already presented a model-based sheet feedback control design, which does take into account disturbances and guarantees an H_∞ performance. Still, the motor dynamics are not included in the control design. Furthermore, during the control design, iterations are needed to realize a desired bandwidth and the controller structure is dependent on the class of sheet setpoint profiles. In this paper we present a structured model-based sheet feedback control design approach, which does take into account motor dynamics as well as the presence of disturbances, which will result in a sheet feedback controller that guarantees performance in the H_∞ sense. Furthermore, it is independent of the setpoint profile of the sheet. As in [4], the control problem is split up into low level motor control loops and a high level sheet control loop. First, the low level motor control loops are designed by using SISO loopshaping techniques. Secondly, the high level sheet control loop is designed while taking into account the controlled low level motor dynamics, such that the control loops are closed sequentially.

The remainder of this paper is organized as follows: in Section 2 the system at hand will be described together with

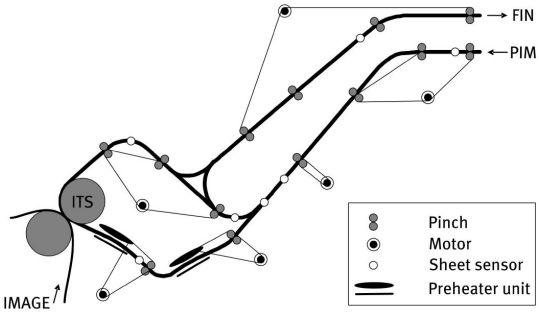

Fig. 1. Example of an industrial printer paper path.

[1] This work has been carried out as part of the Boderc project under the responsibility of the Embedded Systems Institute. This project is partially supported by the Netherlands Ministry of Economic Affairs under the Senter TS program.

Jeroen de Best, Björn Bukkems, René van de Molengraft, and Maarten Steinbuch are with the Dynamics and Control Technology Group, Department of Mechanical Engineering, Technische Universiteit Eindhoven, P.O. Box 513, 5600 MB Eindhoven, The Netherlands, Phone: +31 40 247 4227, Fax: +31 40 246 1418, Email: J.J.T.H.d.Best@tue.nl, B.H.M.Bukkems@tue.nl, M.J.G.v.d.Molengraft@tue.nl, M.Steinbuch@tue.nl

a derivation of the complete high level dynamics. Also the control goal will be given. In Section 3 the control synthesis will be presented, whereas in Section 4 the experimental setup, which is used for validation experiments, will be described. The results of the modeling, control design and experimental validation are presented in Section 5. At the end, conclusions are drawn and recommendations are given.

II. Control problem

Although the paper path depicted in Fig. 1 has many challenging aspects, like for example the coupled pinches and the duplex loop, we consider a more basic printer paper path. By considering this basic paper path, shown in Fig. 2, we obtain insight in the essence of the control problem, which lies in the consecutive switching of the driving pinch. The paper path under consideration consists of three pinches, located at x_{p1}, x_{p2} and x_{p3}, which are all driven by separate motors. The distance between the three pinches is equal to the sheet length L, so sheets cannot be in more than one pinch at the same time. The transmission ratios between motor and pinch are denoted by n_i and the radii of the driven pinches are denoted by R_i, $i \in \mathcal{I}$, with $\mathcal{I} = \{1, 2, 3\}$ the index set of the sheet regions. The angular motor velocities, denoted by $\omega_{mi}(t)$, are measured. No slip is assumed between the sheet and the pinches and the gear belt between the motor and pinches is assumed to be infinitely stiff. The mass of the sheet is assumed to be zero and the sheet position $x_s(t)$, defined as the leading edge of the sheet, is assumed to be known.

As in [1], [2], [4], the control layout is split up into low level motor control loops and a high level sheet control loop, yielding the cascaded control architecture that is schematically depicted in Fig 3. The low level motor control loops consist of low level motor dynamics and low level motor controllers, that together form the controlled low level motor dynamics, here denoted by LLTs. These LLTs map the prescribed angular motor reference velocities $\omega_{mi,r}(t)$ to the actual angular motor velocities $\omega_{mi}(t)$. The high level sheet dynamics (HLP) map the actual angular motor velocities to the sheet position $x_s(t)$. Since at each time instant the sheet is only driven by a single pinch, the input of the high level sheet dynamics will change when the sheet arrives at the next pinch. The pinches that do not contain a sheet are still driven by the high level sheet controller. The complete high level dynamics is the series connection of the controlled low

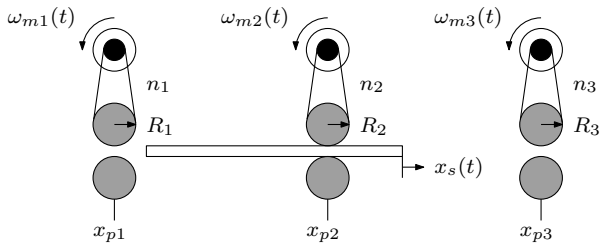

Fig. 2. Basic printer paper path.

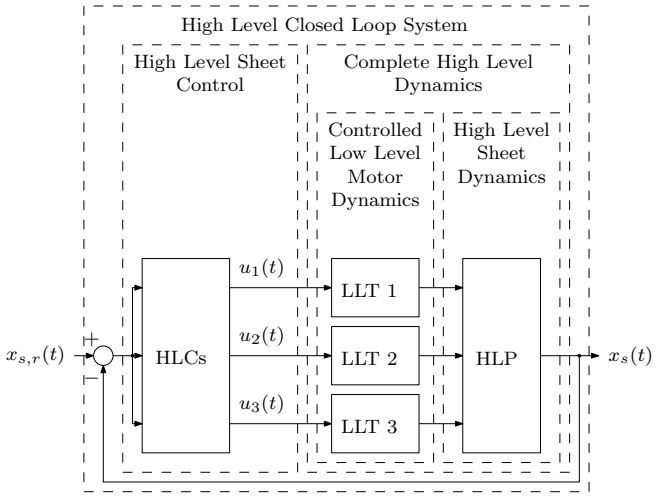

Fig. 3. Block diagram of the total control scheme.

level motor dynamics and the high level sheet dynamics. To describe the switching nature of the system, the complete high level dynamics are formulated in the piecewise linear (PWL) formalism [5]:

$$\begin{matrix} \dot{\underline{x}}_G(t) = A_{Gi}\underline{x}_G(t) + B_{Gi}\underline{u}(t) \\ x_s(t) = C_G\underline{x}_G(t) \end{matrix} , x_s(t) \in \mathcal{X}_i, i \in \mathcal{I}, \qquad (1)$$

where A_{Gi}, B_{Gi} and C_G are the system matrices, input matrices and output matrix of regime i, respectively. The output, the sheet position, does not depend on i. The state vector is defined as $\underline{x}_G(t)$, which contains the angular motor positions, angular motor velocities, low level motor controller states and the sheet position. The input vector is defined as $\underline{u}(t) = [\omega_{m1,r}(t) \;\; \omega_{m2,r}(t) \;\; \omega_{m3,r}(t)]^T$. The partitioning of the state space into the three regions is represented by $\{\mathcal{X}_i\}_{i\in\mathcal{I}} \subseteq \mathbb{R}$. Here, $\mathcal{X}_1 = \{x_s(t)|x_s(t) \in [x_{p1}, x_{p2})\}$, $\mathcal{X}_2 = \{x_s(t)|x_s(t) \in [x_{p2}, x_{p3})\}$ and $\mathcal{X}_3 = \{x_s(t)|x_s(t) \in [x_{p3}, x_{p3} + L)\}$. Since the system under consideration inherently shows piecewise linear behavior the PWL approach is a logical choice. In industrial paper paths, two pinches may be be driving the same sheet over a short time interval. Hence, depending on the pinch velocities, interaction between the pinches is possible which can also be captured in the PWL formalism by introducing extra regimes with different dynamical behavior in the model (1). However, as a first exploration of PWL sheet control design, this paper will focus on the control design of the basic paper path of Fig. 2.

Given the complete high level dynamics (1), the control goal we adopt is the structured design of high level sheet controllers (HLCs) with H_∞ performance that calculate angular reference velocities for the low level motor control loops in order to track a prescribed sheet reference profile $x_{s,r}(t)$.

III. Control synthesis

In this section we present the H_∞ controller design for the complete high level dynamics (1). In the approach presented,

linear H_∞ control design techniques for each subsystem [6] are combined with stability and performance requirements for the switched system. In Fig. 4, the augmented plant, which consists of the complete high level dynamics augmented with weighting filters, is schematically depicted. The exogenous input $w(t)$ of the augmented plant is taken as the sheet reference position $x_{s,r}(t)$. The outputs to be minimized are the weighted sheet position error $z_1(t)$ and the weighted high level sheet control output $\underline{z}_2(t)$. The measured output is the sheet position error $e_s(t)$ and the output of the high level sheet controller is represented by $\underline{u}(t)$. The filter W_e is used to penalize the sheet tracking error, whereas the filter W_u is used to penalize the control outputs. Given the weighting filters together with the complete high level system to be controlled (1), the augmented plant becomes [7]

$$\begin{aligned} \dot{\underline{x}}(t) &= A_i\underline{x}(t) + B_{wi}w(t) + B_i\underline{u}(t) \\ \underline{z}(t) &= C_{zi}\underline{x}(t) + D_{zwi}w(t) + D_{zi}\underline{u}(t),\ i \in \mathcal{I}, \\ e_s(t) &= C\underline{x}(t) + D_{wi}w(t) \end{aligned} \tag{2}$$

where $\underline{x}(t)$ is the state vector containing the angular motor positions, angular motor velocities, low level motor controller states, weighting filter states and the sheet position. Our goal is to compute dynamic high level output-feedback controllers that stabilize the complete high level dynamics (1). Furthermore, the controllers should guarantee performance in the H_∞ sense. This means that, given a prescribed level of disturbance attenuation $0 < \gamma \leq 1$, the induced L_2-norm from $w(t)$ to the controlled outputs, defined as $\underline{z}(t) = \left[z_1(t)\ \underline{z}_2^T(t)\right]^T$, should be smaller than γ under zero initial conditions:

$$\|\underline{z}(t)\|_2 < \gamma\|w(t)\|_2. \tag{3}$$

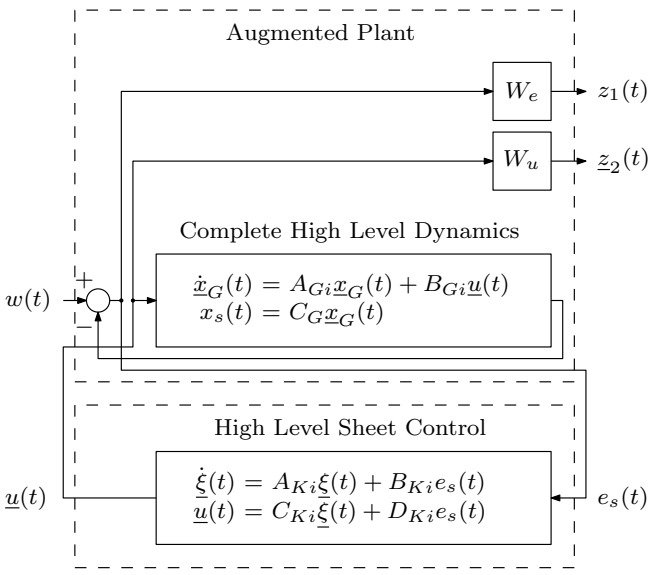

Fig. 4. Augmented plant for the three pinch paper path.

The high level sheet controllers that we propose for achieving this goal are given by

$$\begin{aligned} \dot{\underline{\xi}}(t) &= A_{Ki}\underline{\xi}(t) + B_{Ki}e_s(t) \\ \underline{u}(t) &= C_K\underline{\xi}(t) + D_Ke_s(t) \end{aligned},\ i \in \mathcal{I}, \tag{4}$$

where $\underline{\xi}(t)$ is the controller state, which has the same order as the augmented plant. Substitution of (4) into (2) yields the PWL closed-loop dynamics

$$\begin{aligned} \dot{\underline{x}}_{cl}(t) &= \mathcal{A}_i\underline{x}_{cl}(t) + \mathcal{B}_iw(t) \\ \underline{z}(t) &= \mathcal{C}_i\underline{x}_{cl}(t) + \mathcal{D}_iw(t) \end{aligned},\ i \in \mathcal{I}, \tag{5}$$

with

$$\left(\begin{array}{c|c} \mathcal{A}_i & \mathcal{B}_i \\ \hline \mathcal{C}_i & \mathcal{D}_i \end{array}\right) = \tag{6}$$

$$\left(\begin{array}{cc|c} A_i + B_iD_KC & B_iC_K & B_{wi} + B_iD_KD_{wi} \\ B_{Ki}C & A_{Ki} & B_{Ki}D_{wi} \\ \hline C_{zi} + D_{zi}D_KC & D_{zi}C_K & D_{zwi} + D_{zi}D_KD_{wi} \end{array}\right).$$

In literature, several techniques for proving stability of PWL systems are available [8], [9], [10], [11]. However these results only encompass stability or stabilization via state feedback of PWL systems and lack controller synthesis via output feedback. Therefore, in this case we aim at proving stability by adopting a common quadratic Lyapunov function for all regions. The expectation is that conservatism does not negatively influence the control synthesis, since the dynamics in each of the regions are approximately the same. So if the closed-loop system (5) admits a common quadratic Lyapunov function

$$V(\underline{x}_{cl}(t)) = \underline{x}_{cl}^T(t)\mathcal{P}\underline{x}_{cl}(t) > 0, \tag{7}$$

such that

$$\mathcal{A}_i^T\mathcal{P} + \mathcal{P}\mathcal{A}_i < 0,\ i \in \mathcal{I}, \tag{8}$$

then the controllers are stabilizing [7]. The closed-loop system is stable and has an H_∞ norm smaller than γ if there exists a symmetric $\mathcal{P}$ with

$$\mathcal{P} > 0, \tag{9}$$

$$\left(\begin{array}{ccc} \mathcal{A}_i^T\mathcal{P} + \mathcal{P}\mathcal{A}_i & \mathcal{P}\mathcal{B}_i & \mathcal{C}_i^T \\ \mathcal{B}_i^T\mathcal{P} & -\gamma I & \mathcal{D}_i^T \\ \mathcal{C}_i & \mathcal{D}_i & -\gamma I \end{array}\right) < 0,\quad i \in \mathcal{I}. \tag{10}$$

Equations (9), (10) are matrix inequalities in the variables $\mathcal{P}$, A_{Ki}, B_{Ki}, C_{Ki}, D_{Ki} and γ, $i \in \mathcal{I}$ [7]. By partitioning $\mathcal{P}$ and $\mathcal{P}^{-1}$ as

$$\mathcal{P} = \left(\begin{array}{cc} Y & N \\ N^T & * \end{array}\right),\quad \mathcal{P}^{-1} = \left(\begin{array}{cc} X & M \\ M^T & * \end{array}\right), \tag{11}$$

where X and Y are $n \times n$ symmetric matrices, and by using the linearizing change of variables given in [7]

$$\begin{aligned} \widehat{A}_i &= NA_{Ki}M^T + NB_{Ki}CX + \\ &\quad + YB_iC_KM^T + Y(A_i + B_iD_KC)X \\ \widehat{B}_i &= NB_{Ki} + YB_iD_K \\ \widehat{C} &= C_KM^T + D_KCX \\ \widehat{D} &= D_K \end{aligned} \quad ,i \in \mathcal{I}, \tag{12}$$

$$\begin{pmatrix} A_iX + XA_i^T + B_i\widehat{C} + (B_i\widehat{C})^T & * & * & * \\ \widehat{A}_i + (A_i + B_i\widehat{D}C)^T & A_i^TY + YA_i + \widehat{B}_iC + (\widehat{B}_iC)^T & * & * \\ (B_{wi} + B_i\widehat{D}D_{wi})^T & (YB_{wi} + \widehat{B}_iD_{wi})^T & -\gamma I & * \\ C_{zi}X + D_{zi}\widehat{C} & C_{zi} + D_{zi}\widehat{D}C & D_{zwi} + D_{zi}\widehat{D}D_{wi} & -\gamma I \end{pmatrix} < 0, \quad i \in \mathcal{I}$$

$$\begin{pmatrix} X & I \\ I & Y \end{pmatrix} > 0 \tag{13}$$

the matrix inequalities (9) and (10) can be reformulated as linear matrix inequalities (LMIs) with free variables X, Y, $\widehat{A}_i$, $\widehat{B}_i$, $\widehat{C}$, $\widehat{D}$ and γ, $i \in \mathcal{I}$, see (13). If these LMIs are found to be feasible, nonsingular matrices M and N, satisfying the relation $MN^T = I - XY$, can be calculated using a singular value decomposition. Afterwards, the controller matrices can be calculated from (12) in reversed order.

IV. Experimental setup

To validate the proposed control design, the experimental printer paper path setup as shown in Fig. 5 is used. It consists of a paper input module and a paper path with five pinches. In the experiments the second, third and fourth pinch are the pinches where the actual control action takes place. In the remainder of this paper we will refer to these pinches as pinch $p1$, pinch $p2$, and pinch $p3$ respectively. Each pinch is connected to a motor via a gear belt. The transmission ratios are $n_1 = \frac{18}{37}$, $n_2 = \frac{16}{30}$ and $n_3 = \frac{18}{37}$. The radii R_i of the pinches are $14{\cdot}10^{-3}$ m. The angular positions of the motors are measured via optical incremental encoders with a resolution of 2000 increments per revolution. The motors are 10 W DC motors driven by current amplifiers. Both the amplifiers and the encoders are connected to a PC-based control system. This system consists of three TUeDACS USB I/O devices [12], a Pentium 4 host computer running RTAI/Fusion Linux and Matlab/Simulink. The sheets are guided through the paper path using thin steel wires and their position is measured using optical mouse sensors with a resolution of approximately 10 μm, which are directly connected to the host computer via USB.

V. Results

In this section the results regarding the modeling of the complete high level dynamics (1) will be given first.

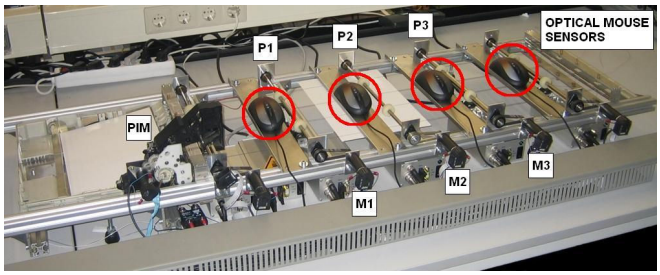

Fig. 5. The experimental printer paper path setup.

Furthermore, the design of the weighting filters W_e and W_u and the resulting high level sheet controllers will be presented, followed by the results of the experiments.

A. Complete High Level Dynamics

1) Controlled low level motor dynamics: The low level motor dynamics are modeled as double integrators

$$\frac{\Phi_{mi}(s)}{V(s)} = \frac{K_{Ai}K_{Mi}}{J_is^2}e^{-\theta s}, i \in \mathcal{I}, \tag{14}$$

where K_{Ai} are the amplification factors of the current amplifiers in AV^{-1}, K_{Mi} are the motor constants in NmA^{-1}, J_i are the inertias of the low level systems in kgm^2, and θ is the delay time in seconds. $\Phi_{mi}(s)$ and $V(s)$ are the Laplace transforms of the motor position $\phi_{mi}(t)$ and the motor input $V(t)$, respectively. The amplification factors of the used current amplifiers are identified as $K_{A1} = 0.54$ AV^{-1}, $K_{A2} = 0.51$ AV^{-1} and $K_{A3} = 0.53$ AV^{-1}. From specifications we know that the motor constant is $4.38{\cdot}10^{-2}$ NmA^{-1} for each motor. The inertias of the low level systems are determined from frequency response function (FRF) measurements and are $J_1 = 2.9{\cdot}10^{-6}$ kgm^2, $J_2 = 3.3{\cdot}10^{-6}$ kgm^2 and $J_3 = 2.9 \cdot 10^{-6}$ kgm^2. From the FRFs we know that the delay time, mostly present due to the digital implementation of the control scheme is $1.5 \cdot 10^{-3}$ seconds in every low level control loop. This delay is approximated by a second order Padé approximation [6]

$$e^{-\theta s} \approx \frac{(1 - \frac{\theta}{4}s)^2}{(1 + \frac{\theta}{4}s)^2}. \tag{15}$$

Due to the high stiffness in the gear belt between the motor and pinch, flexibilities in the drive line manifest themselves at high frequencies. From FRFs we know that these frequencies are around 400 Hz. These flexibilities are not bandwidth limiting and are therefore not taken into account in the modeling of the low level motor dynamics. Including this phenomenon would result in a higher order of the complete high level dynamics and therefore in a higher order of the controller, since the order of the controller is the same as the order of the augmented plant.

Using standard loop shaping techniques [13], low level controllers have been designed for each motor. They consist of a lead filter in combination with an integral action. The lead filters are designed with the zero at $1/4 \cdot 50$ Hz and the pole at $4 \cdot 50$ Hz. The cut-off frequency of the integral action is $1/5 \cdot 50$ Hz. The resulting crossover frequencies are approximately 50 Hz. Since the low level controllers

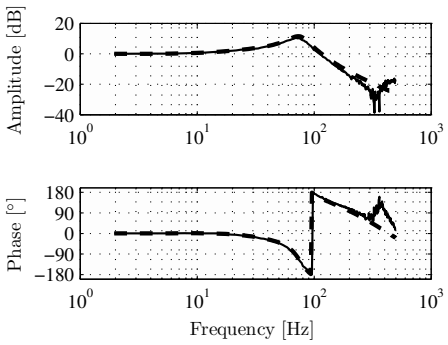

Fig. 6. FRF (solid) together with the model (dashed) of the complementary sensitivity of motor 1.

use the motor positions for feedback the output of the high level sheet controllers is integrated to obtain angular motor reference positions.

From the low level motor dynamics and the low level motor controllers the controlled low level motor dynamics (LLTs) can be derived

$$\frac{\Omega_{mi}(s)}{\Omega_{mi,r}(s)} \quad = \quad T_i(s), i \in \mathcal{I}, \tag{16}$$

with $\Omega_{mi,r}(s)$ the Laplace transform of the angular motor reference velocities $\omega_{mi,r}(t)$. The result of the modeling can be seen in Fig. 6, which shows the FRF and the model of the complementary sensitivity function of the first LLT. As can be seen the motor perfectly tracks the prescribed reference velocities until approximately 10 Hz. For higher frequencies this ideal behavior is lost. The flexibilities at 400 Hz due to the limited belt stiffness can also be observed in this figure. Similar results are obtained for the second and third low level system.

2) High level sheet dynamics: As in [4], the high level sheet dynamics are given by the following PWL model

$$\dot{x}_s(t) = B_i \left[\omega_{m1}(t) \;\; \omega_{m2}(t) \;\; \omega_{m3}(t)\right]^T, x_s(t) \in \mathcal{X}_i, i \in \mathcal{I}, \tag{17}$$

with the input matrices B_i defined as $B_1 = [n_1 R_1 \; 0 \; 0]$, $B_2 = [0 \; n_2 R_2 \; 0]$ and $B_3 = [0 \; 0 \; n_3 R_3]$. This model can be seen as a switching integrator.

Given the model of the high level sheet dynamics (17) together with the models of the controlled low level motor dynamics (16), the complete high level dynamics (1) are known and the control design can be carried out.

B. Control Design

Before calculating the high level controllers, the weighting filters W_e and W_u have to be designed. The weighting filter W_e is used to shape the sensitivity function S. With W_e we can enforce both a desired bandwidth and an integral action in the high level sheet controllers. This is done by designing the weighting filter as

$$W_e(s) \; = \; \frac{1}{S_0} \frac{\frac{1}{4\pi^2 f_{BW} f_I} s^2 + \left(\frac{0.7}{2\pi f_{BW}} + \frac{0.7}{2\pi f_I}\right) s + 1}{\frac{S_\infty}{4\pi^2 S_0 f_{BW} f_I} s^2 + \frac{2 \cdot 0.7 \sqrt{S_\infty}}{2\pi \sqrt{S_0 f_{BW} f_I}} s + 1}. \tag{18}$$

Here, f_{BW} is the desired bandwidth and f_I is the desired cut-off frequency of the integral action. The values of f_{BW} and f_I are chosen to be 15 Hz and 3 Hz, respectively. S_0 is the desired asymptotic amplitude of the sensitivity when $f \to 0$ and S_∞ is the desired asymptotic amplitude of the sensitivity when $f \to \infty$. These values are chosen as $S_0 = 10^{\frac{-150}{20}}$ and $S_\infty = 10^{\frac{6}{20}}$. For low frequencies the weighting filter has a slope of zero in order to prevent inserting a pole in $f = 0$ in the augmented plant which cannot be stabilized by the controller. For mid range frequencies up to f_I, a -2 slope is present. This corresponds to a desired -1 slope of the high level sheet controller caused by the integral action multiplied with the -1 slope of the complete high level dynamics in that frequency range.

The weighting filter W_u is used to shape the control sensitivity function S_C. W_u is selected to represent a matrix with a SISO weighting filter w_u on each diagonal element and with zeros on all other elements. By weighting each control input with the weighting filter given by

$$w_u(s) \; = \; \frac{\frac{1}{2\pi f_{LP}} s + 1}{\frac{C_\infty}{2\pi f_{LP}} s + C_0}. \tag{19}$$

a high frequency roll-off can be enforced in the controller. Here f_{LP} is the desired roll-off frequency, C_0 is the desired asymptotic amplitude of the control sensitivity when $f \to 0$ and C_∞ is the desired asymptotic amplitude of the control sensitivity when $f \to \infty$. The values are chosen as $f_{LP} = 50$ Hz, $C_0 = 10^{\frac{100}{20}}$ and $C_\infty = 10^{\frac{-40}{20}}$. Since $S \approx 1$ for frequencies far above the bandwidth, we can approximate the control sensitivity S_C by the controller in this region. So for high frequencies we are weighing the controller and therefore the desired roll-off can be shaped.

Given the complete high level dynamics (1) and the weighting filters (18) and (19), the linear matrix inequalities (13) are solved using the LMI Control Toolbox [14]. By setting $\gamma = 1$ and solving a feasibility problem, stable high level sheet controllers were obtained. The results of the control design are given in the Figs. 7 and 8. In Fig. 7 the obtained controller is depicted for the first subsystem. It can be seen that the desired integral action and roll-off are indeed present. The obtained crossover frequency of 10 Hz can be seen in Fig. 8, which shows the loop gain of the first subsystem. Similar results are obtained for the second and third subsystem.

C. Experiments

To experimentally validate the control design in practice, experiments are carried out. For the sheets motion task, a constant velocity of 0.3 ms^{-1} is chosen that has to be tracked throughout the paper path. The corresponding sheet reference motion is therefore a ramp function. The results of the experiment can be seen in Fig. 9. When the sheet enters the paper path, the pinches are standing still. Due

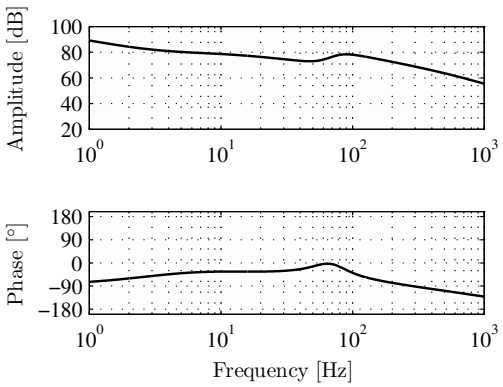

Fig. 7. Designed high level sheet controller.

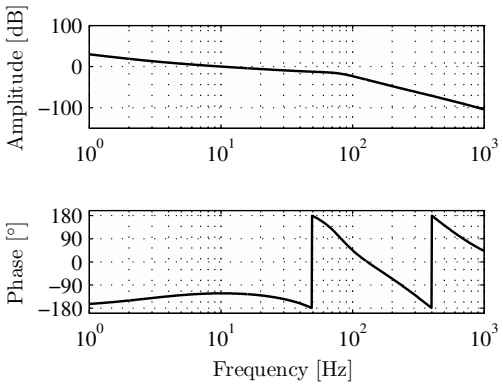

Fig. 8. Designed high level open loop.

to the nonzero reference velocity at that moment the error starts to increase. However, this error is quickly decreased by the controller. From Fig. 9 we observe that the closed-loop system is stable. Furthermore, it can be seen that there is a close match between the experimentally obtained tracking error and the results obtained from simulation, which justifies the assumption of an infinitely stiff coupling between motor and pinch.

VI. Conclusions and Recommendations

In this paper, a structured model-based control design approach for sheet control in a printer paper path has been presented, which guarantees performance in the H_∞ sense. By taking into account the low level dynamics we have incorporated the bandwidth limiting factor into the design of the high level sheet controllers. With the use of optical mouse sensors the sheet position is made available in experiments, enabling an experimental validation of the control design. These experiments show closed-loop stability. Furthermore, they inherently show robustness against parameter uncertainties. Future research will focus on the extension

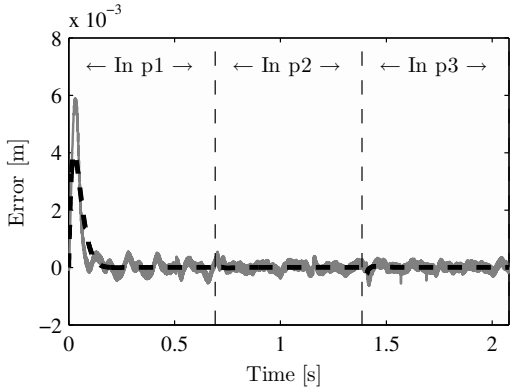

Fig. 9. Experimentally obtained error (solid) together with error obtained from simulation (dashed).

of the augmented plant by including weighting filters for uncertainties in order to create a robust controller with H_∞ performance. Furthermore, control design for configurations where the pinches are coupled into sections and for paper paths with a duplex loop are subject of future research.

References

[1] C. Cloet, "A mechatronics approach to copier paperpath design," Ph.D. dissertation, University of California Berkely, CA, USA, 2001.

[2] M. Kruciński, "Feedback control of photocopying machinery," Ph.D. dissertation, University of California Berkely, CA, USA, 2001.

[3] S. Rai, "A hybrid hierarchical control architecture for paper transport systems," *Proc. 1998 IEEE CDC*, vol. 4, pp. 4294–4295, March 1998.

[4] B. Bukkems, J. de Best, R. van de Molengraft, and M. Steinbuch, "Robust piecewise linear sheet control in a printer paper path," *2nd IFAC Conference on Analysis and Design of Hybrid Systems (ADHS '06)*, June 2006.

[5] E. Sontag, "Nonlinear regulation: The piecewise linear approach," *IEEE Trans. on Autom. Contr.*, vol. 26, no. 2, pp. 346–358, April 1981.

[6] S. Skogestad and I. Postlethwaite, *Multivariable Feedback Control Analysis and Design*, 2nd ed. The Atrium, Southern Gate, Chichester, West Sussex PO19 8SQ, England: John Wiley & Sons Ltd, 2005.

[7] C. Scherer, P. Gahinet, and M. Chilali, "Multiobjective output-feedback control via LMI optimization," *IEEE Trans. on Autom. Contr.*, vol. 42, no. 7, pp. 896–911, July 1997.

[8] M. Johansson and A. Rantzer, "Computation of piecewise quadratic lyapunov functions for hybrid systems," *IEEE Trans. on Autom. Contr.*, vol. 43, no. 4, pp. 555–559, April 1998.

[9] A. Hassibi and S. Boyd, "Quadratic stabilization and control of piecewise-linear systems," *Proc. 1998 ACC*, vol. 6, pp. 3659–3664, June 1998.

[10] S. Boyd, L. Ghaoui, E. Feron, and V. Balakrishnan, *Linear matrix inequalities in systems and control theory*. Philadelphia: SIAM Society for industrial and applied mathematics, 1994, vol. 15.

[11] G. Feng, G. Lu, and S. Zhou, "An approach to $\mathcal{H}_\infty$ controller synthesis of piecewise linear systems," *Communications in information and systems*, vol. 2, no. 3, pp. 245–254, December 2002.

[12] R. van de Molengraft, M. Steinbuch, and B. de Kraker, "Integrating experimentation into control courses," *IEEE Control Systems Magazine*, vol. 25, no. 1, pp. 40–44, February 2005.

[13] G. Franklin, J. Powell, and A. Emami-Naeini, *Feedback control of dynamic systems*, 3rd ed. Reading, Massachusetts: Addison-Wesley Publishing Company, 1994.

[14] P. Gahinet, A. Nemirovskii, A. Laub, and M. Chilali, "The LMI control toolbox," *Proc. 1994 IEEE CDC*, vol. 3, pp. 2038–2041, December 1994.